Mathematical Biology and Bioinformatics. 2014. V. 9. № 2. P. 464–481.
URL: http://www.matbio.org/2014/Ustinin_9_464.pdf.

========== **DATA MINING** ==========

UDC: 612.825.5+004.925

New Methodology for the Analysis and Representation of Human Brain Function: MEGMRIAn

Ustinin M.N.[1,2,3], Sychev V.V.[1], Walton K.D.[2], Llinás R.R.[2]

[1]*Institute of Mathematical Problems of Biology RAS, Pushchino, 142290, Russian Federation*
[2]*New York University, NY, 10016, USA*
[3]*Pushchino State Institute of Natural Sciences, Pushchino, 142290, Russian Federation*

Abstract. The present software was developed to implement a highly spatiotemporal resolved functional tomography (1mm/1msec), capable of addressing spontaneous and evoked activity at any point in the human brain. Presently the methodology is implemented for the magnetic encephalography data. Data analysis results are embedded into a magnetic resonance image of the head. This image is also used as the head model to calculate the magnetic fields of the equivalent current dipoles, while probe positions correspond to real device coordinates. This methodology allows the superposition of the functional frequency patterns to be represented together with magnetic resonance images. The software computational speed makes it possible to implement the whole data acquisition and imaging cycle fast enough to allow optimal protocol choice in data processing.

Key words: *magnetic encephalography, spontaneous and evoked brain activity, inverse problem solution, spectral analysis, functional tomography.*

INTRODUCTION

Magnetoencephalography (MEG) records the magnetic fields generated by the electrical currents of brain neurons. The method was developed because the magnetic signal is not distorted as it passes through the overlying soft tissue and skull and thus provides a more accurate measurement of brain activity than the electrical signal (EEG) that is distorted as it leaves the brain. A non-invasive technology, MEG employs highly sensitive superconducting quantum interferometers (SQUIDS) to record activity at a femtotesla-level ($<10^{-15}$ T). The sampling frequency can be quite high (up to several thousand Hz) providing a temporal resolution of fractions of a millisecond. Magnetic resonance imaging (MRI) of the head provides complementary information about brain structure. In principle, combined MEG and MRI information can provide spatiotemporal resolution on a millimeter and millisecond scale. MEG instruments record magnetic fields from hundreds of channels uniformly distributed over the head surface, producing large experimental data arrays. Such multichannel spatiotemporal magnetic fields have been analyzed using various mathematical methods [1].

One of the predominant issues concerning MEG recordings belongs to a group of mathematical problems called ‘inverse problems’. In this application, the observed measurements of brain activity (MEG data) must be converted into information about the localization of current dipole sources of such activity using a mathematical model. Many approaches have been taken to solving the MEG inverse problem [2, 3]. In this paper we present a unique solution to the inverse problem that allows the reconstruction of the spatial structure of activity dipole sources on an MRI.

In a typical study of the spontaneous brain activity, about 100 million field values are recorded (275 channels registered for 420 seconds with sampling rate 1200 Hz, produce 1.386×10^8 samples). These records require powerful software and hardware processing. The state of the art in this field was recently reviewed by Baillet and colleagues [3]. A large

variety of software types have been developed. Some address conventional methods, other are oriented to solve problems for particular human neurobiological issues. Eight are summarized here: 1) FieldTrip is software that supports analysis of both magneto- and electroencephalographic data [4]. This software, written in MATLAB, provides a set of high-level functions for data processing, including algorithms for time-frequency analysis (multitapers) and for the reconstruction of dipolar and distributed sources. 2) Brainstorm, open-source software for MEG processing/visualization, is directed toward cortical source estimation and allows anatomical registration providing excellent MEG localization methods in an intuitive user-friendly interface [5]. 3) ELAN presents a wide range of tools to analyze electrophysiological data, especially in evoked responses, while not localizing the sources [6]. 4) HADES gives an estimation of current dipoles from the biomagnetic data, where the number and location of dipoles is changing dynamically depending on the magnetic encephalogram [7]. This software is controlled through the graphic user interface, but also does not include localization of the sources. 5) OpenMEEG provides program for the realistic physiological modelling of electromagnetic fields produced by the brain sources. Instantaneous values of the EEG and MEG are calculated [8]. 6) rtMEG is a hardware and software complex for the real-time encephalographic analysis, making it possible to inform the subject about his brain activity during the recording [9]. 7) The program package EMEGS provides various methods to process and analyze encephalograms, while not representing sources on the MRI [10]. 8) A wide spectrum of methods to process the MEG is provided by the NUTMEG software, including graphic representation of sources on an MRI [11].

Our program package, MEGMRIAn, was developed to process and analyze MEG data. This program was developed using data obtained at the Center for Neuromagnetism in the Department of Neuroscience and Physiology at the New York University School of Medicine. Studies in this laboratory have addressed spontaneous and evoked brain activity under both physiological (12-16) and pathophysiological [17-19] conditions. Authors were participating in the development of new methods of data analysis [20–22], included in the MEGMRIAn software and verified on the experimental data.

Recently, we proposed using precise frequency-pattern analysis to decompose complex systems into functionally invariant entities [23, 24]. This method makes it possible to address general spectra to the partial spectra of stable functional entities and to restore their time series. The method is based on the complete utilization of the long time series, while the multichannel nature of the data is also completely taken into account making it possible to implement the detailed reconstruction of neuronal circuit activity. This methodology has also been applied to the analysis of MEG with high-level noise, making it possible to extract an auditory response [25]. The new version of the MEGMRIAn software presented here incorporates the application of precise frequency-pattern analysis to the functional structure of the human brain.

THE GENERAL STRUCTURE OF THE MEGMRIAn SOFTWARE

The first draft of the software was launched in 2002 when the general layout of the program, comprising separate windows each solving a different problem, was designed [26]. Data exchange between the windows was performed through the random access memory or, for large data sets, through disk storage. As software development advanced, the composition of data processing methods changed and new functions and windows were added. The newest version of the software has been named MEGMRIAn 5.14, short for «MEG and MRI integrated Analysis, version 5.14», where 5 represents the number of windows, and 14 the release year.

The program package includes 160 MATLAB functions, with over 1200 lines of code. It is an interactive graphic environment for the analysis and combined visualization of

magnetoencephalographic data (MEG), magnetic resonance images (MRI), multichannel spectra (MS) and functional tomograms (FT).

MEGMRIAn 5.14 makes it possible to:

- read files containing MRT, MEG, MS, FT and time series,
- remove channels with artifacts from MEG,
- choose a data segment to be analyzed in detail,
- identify a useful signal in MEG,
- perform amplitude mapping of the MEG or MS,
- solve the forward problem in one- or two-dipole models,
- solve the inverse problem in one- or two-dipole models,
- construct sections of the tomogram through the dipole position,
- represent inverse problem solution on tomographic sections,
- assess the reliability of the dipole sources found,
- estimate coherence of the selected frequency,
- restore the MEG at the selected frequency,
- represent FT over the MRI,
- represent FT conjugated with MRI,
- save and print the images obtained,
- make video clips of the sequence of inverse problem solutions.

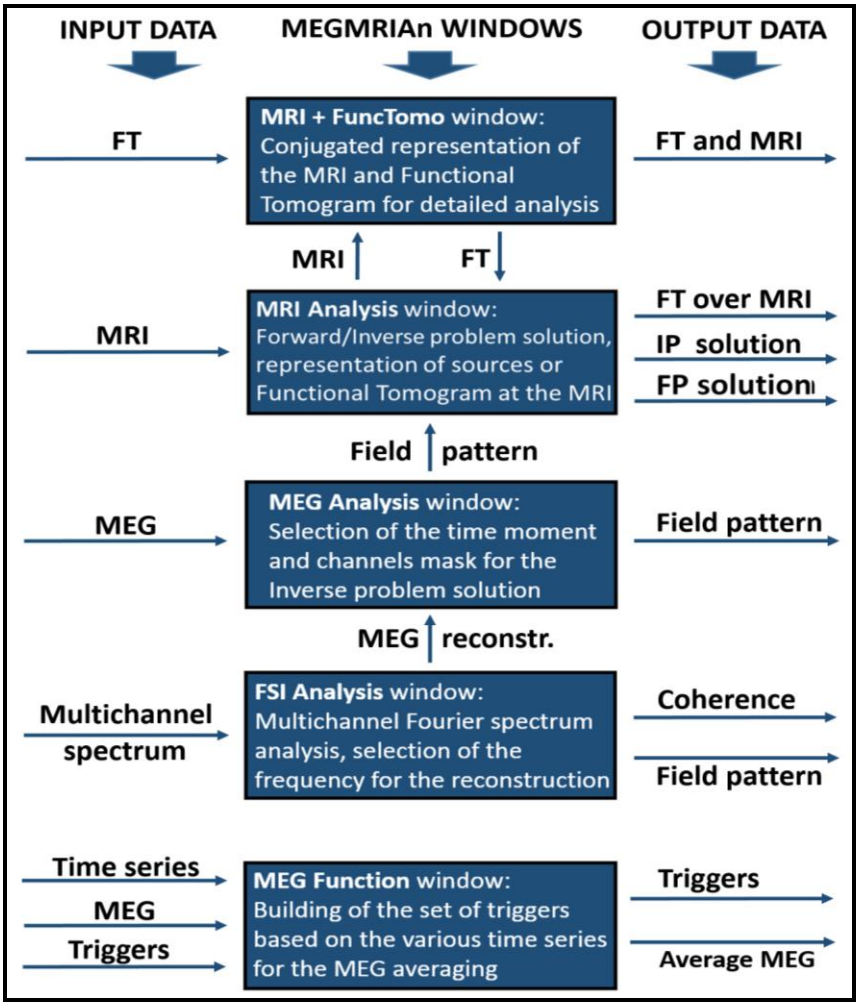

Fig. 1. Block diagram and basic data flow of the MEGMRIAn 5.14 software. MEG – Magnetic Encephalogram; FT – Functional Tomogram; MRI – Magnetic Resonance Image; FSI – Fourier Spectrum Imaging; IP – Inverse Problem; FP – Forward Problem.

The software includes five main windows: **«MRI Analysis»**, **«MEG Analysis»**, **«MEG Function»**, **«FSI Analysis»** and **«MRI + FuncTomo»**. Each window contains the same **Menu** line and is shown separately. The general block diagram of the program and main data flow are given in Figure 1.

In this article all five windows and the boxes they contain will be considered, briefly describing their functions, structure, data exchange and basic protocols of the data analysis.

THE «FSI-Analysis» WINDOW

This window provides a graphic user interface for the analysis of multichannel Fourier spectrum, calculated in frames of precise frequency-pattern analysis method [23, 24]. This method is characterized by the following:

1. Precise calculation of the Fourier integrals. For *i*-th channel the experimental set of points is interpolated, converting it to a continuous function $\tilde{B}_i(t)$. Gaussian quadrature formulas are used to calculate integrals on any interval [0, *T*], in the registration scale: $a_{ni} = \frac{2}{T}\int_0^T \tilde{B}_i(t)\cos(2\pi\nu_n t)\,dt$, $b_{ni} = \frac{2}{T}\int_0^T \tilde{B}_i(t)\sin(2\pi\nu_n t)\,dt$, where a_{ni}, b_{ni} are Fourier coefficients for the frequency ν_n in the channel number i, and $n = 1,...,N$, where $N = \nu_{\max} T$, $\nu_{\max}$ is the highest desirable frequency.

2. Building all spectra for the total registration time *T*, as opposed to methods using moving or fractional window. The step in frequency is: $\Delta\nu = \nu_n - \nu_{n-1} = \frac{1}{T}$, thus frequency resolution is determined by the recording time.

3. Tuning of the frequency grid by cutting the interval of integration *T* to build the optimal approximation of the frequency selected. Tuning can be performed by little changes of the integration time, *T*.

This precise transform leads to an accurate and reversible representation of time data in the frequency domain for each channel. As for the space domain, "space" is determined by data recorded in many channels, having different positions with respect to the source. That is, if an accurate representation of time series for all channels is used, the spatial characteristics of the signal can also be determined accurately.

The window «FSI-analysis» makes it possible to study detailed frequency structure of the system. The multichannel signal is restored at the selected frequency, and the pattern obtained is analyzed. Magnetic induction in channel *i*, restored at the *n*-th frequency, can be written as:

$$B_{ni}(t) = \rho_{ni}\sin(2\pi\nu_n t + \varphi_{ni}), \quad (1)$$

where $\rho_{ni} = \sqrt{a_{ni}^2 + b_{ni}^2}$, $\varphi_{ni} = \operatorname{atan2}(a_{ni}, b_{ni})$, $t \in [0, T_{\nu_n}]$, $T_{\nu_n} = \frac{1}{\nu_n}$.

The summary instantaneous power produced by all channels will be:

$$p_n(t) = \sum_{i=1}^{K} B_{ni}^2(t).$$

Empirical one-frequency coherence of the sources at this frequency can be characterized by the value of phase coincidence, scaling from 1 to 0:

$$C_\nu = 1 - \frac{\min(p(t))}{\max(p(t))},$$

where minimum and maximum are calculated at the period T_{ν_n}. C_ν, therefore, is a value between 0 and 1, inclusive. The physical sense of C_ν follows from (1): C_ν is equal to 1, if all channels have equal phases at the frequency ν_n.

Invariant patterns can be extracted from the signals where there is a high coherence. It was shown in two theorems [23, 24]:

Coherence Theorem 1. The equality of phases in all channels is a necessary and sufficient condition for pattern invariance through the reconstructed time.

Conclusion 1. If, for particular frequency, phases are equal in all channels, then the spatial structure of the source at this frequency can be found by the solution of the inverse problem for the normalized pattern, which is constant throughout the period.

Coherence Theorem 2. Phases equality in all channels is a necessary and sufficient condition for $C_\nu = 1$. This theorem provides a directly calculable feature to estimate the coherence at any frequency ν.

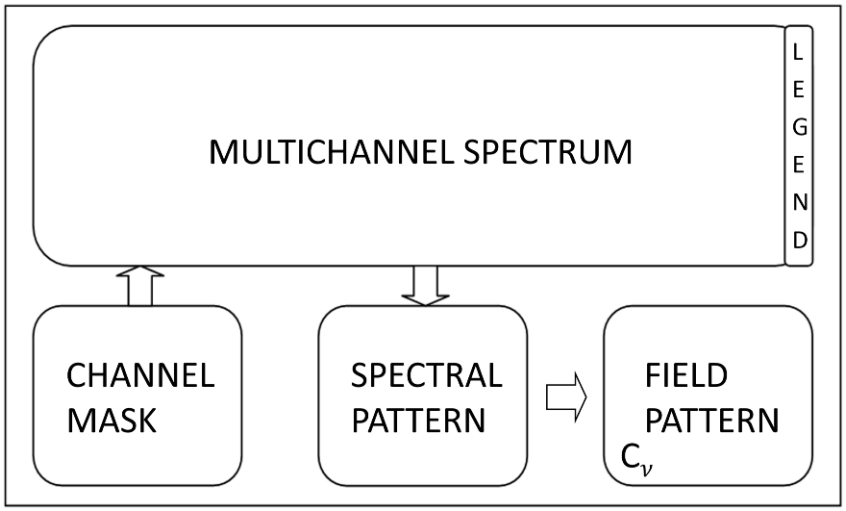

Fig. 2. Block diagram of the «FSI-Analysis» window.

Figure 2 shows a block diagram of the «FSI-Analysis» window. The «Multichannel spectrum» box shows Fourier spectrum amplitude as a function of frequency in active channels, selected in box «Channel mask». Usually, precise spectrum contains many thousands of frequencies, so the box «Multichannel spectrum» allows two views of the spectrum.

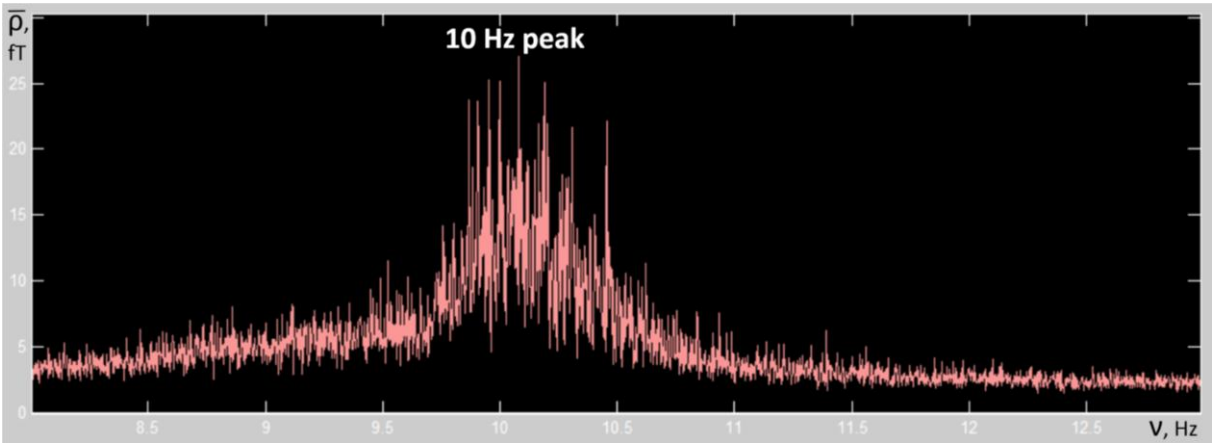

Fig. 3. Average MEG Fourier amplitude as a function of frequency.

If there are more than 2000 frequencies, only one plot of average MEG amplitude is represented. Figure 3 illustrates the spectrum near 10 Hz (alpha rhythm).

Zooming of this box near the highest amplitudes switches the view to a detailed presentation of the multichannel spectrum, where spectra in all channels are shown

simultaneously (Fig. 4). The box «Spectral pattern» shows a Fourier amplitude map at the selected frequency, with mapping legend shown near the spectrum. The «Field pattern» box shows the map of the MEG, restored at the selected frequency. This map corresponds to the moment of maximal instant power. One-frequency coherence value is included in this box.

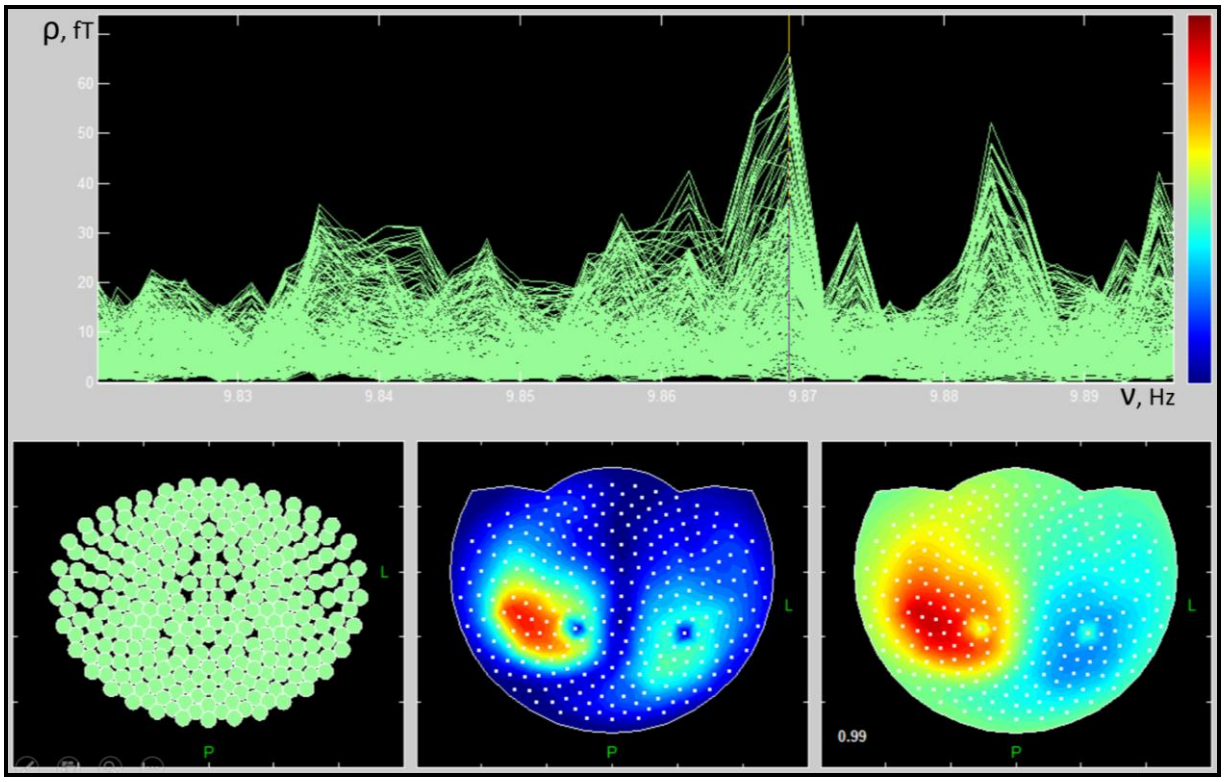

Fig. 4. General view of the window «FSI-Analysis». The vertical line near 9.87 Hz indicates the frequency that was selected for detail analysis. The coherence is equal to 0.99, indicating a very clear single-source oscillation.

In a previous study [23] it was shown, that many precise frequencies reveal very high coherences, making it possible to study the functional structure of the brain. Figure 4 presents an example of such coherent frequency. Further analysis of this frequency will be demonstrated in windows «MEG-Analysis» and «MRI-analysis». The input data for the «FSI-Analysis» window is a precise multichannel Fourier spectrum, calculated by external programs [27, 28]. The output data is the spectrum at the selected frequency. From this spectrum, the magnetoencephalogram is restored in all channels, and the program can be switched to the window «MEG Analysis». After selection of the restored time moment, the spatial structure of the sources can be estimated in the «MRI Analysis» window.

THE «MEG-Analysis» WINDOW

This window is intended to process the MEG time sequence and shows all channels simultaneously (butterfly plot). The input data can be: raw MEG data, a modeled MEG time sequence or the results restored by the inverse Fourier transform from the multichannel spectrum. The output of this window is a magnetic field pattern at the time moment selected by the user. This pattern is transferred to the window «MRI-analysis» to be used for solving the inverse problem.

The block diagram and screenshot of the «MEG-analysis» window are shown in Figures 5 and 6.

MEG samples from the active channels are represented as linearly interpolated curves in the box «Multichannel MEG». The box «Channel mask» makes it possible to select the set of active channels. The box «Input field pattern» presents the instant MEG values at the moment

of time selected with the help of graphic user interface (GUI). The box «Output field pattern» shows the MEG values obtained from inverse or direct problem solution. The mask is always shown as an ordinary diagram, while the input/output MEG values are shown using the amplitude mapping. The correspondence of field value and color is displayed at the box «Legend».

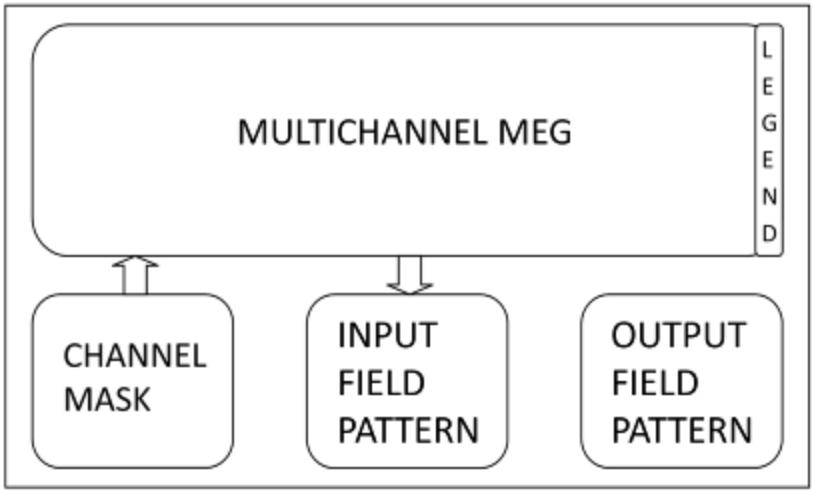

Fig. 5. Block diagram of the «MEG-Analysis» window.

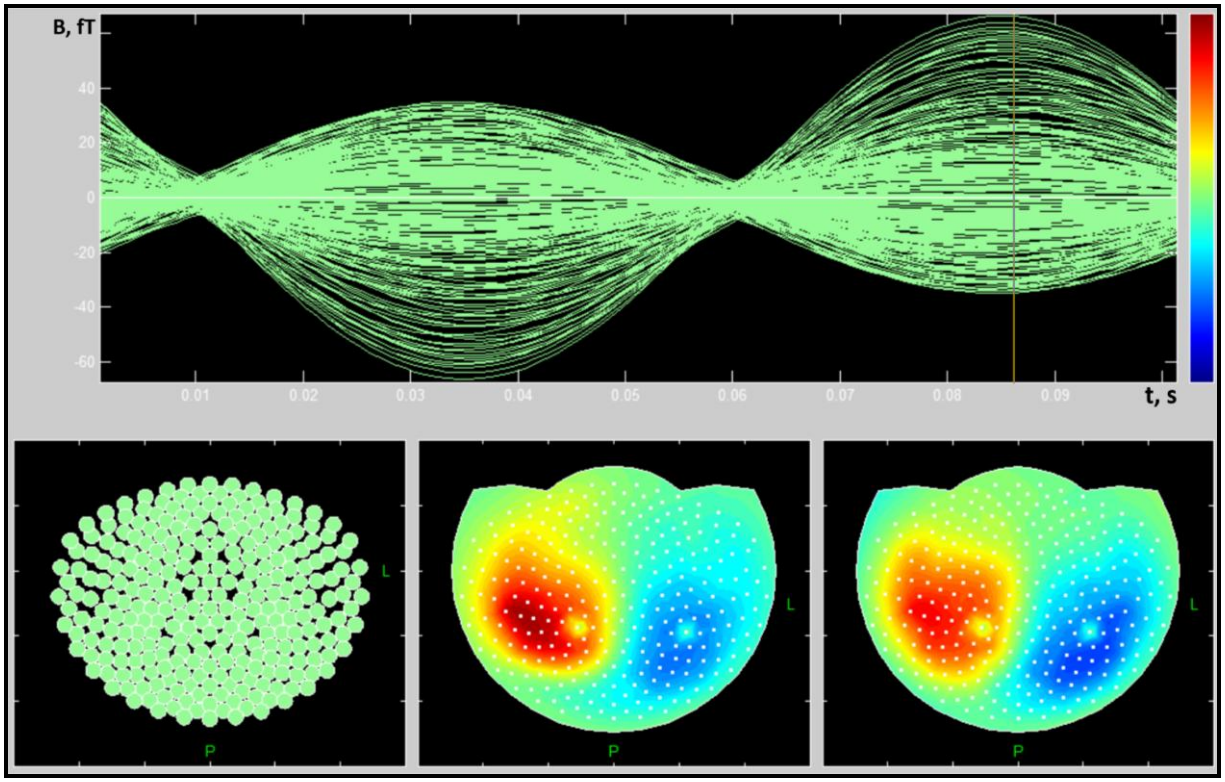

Fig. 6. Typical view of the «MEG» window. The butterfly plot shows multichannel MEG restored from the frequency selected at Fig. 4. Left field map corresponds to the time moment, selected by the vertical line. Right field map presents a solution of the inverse problem (Fig. 10).

Removing of the artifact MEG channels

This procedure can be activated from the menu item «Options–FilterMask». Filtered out channels have zero weight and are not included in dipole fitting and cannot be used in primary mask. Artifact channels are determined from the power distribution between channels: $\sigma_i^2 = \sum_{t=1}^{T} \left(B_i^0(t) \right)^2 / T$, where $B_i^0(t)$ is MEG in i-th channel, T – number of samples. Also the

spatial location of sensors is taken into account. For *i*-th sensor the median $\bar{\sigma}_i$ is calculated from σ_i and the four nearest sensors. If $\sigma_i > 3\bar{\sigma}_i$, then *i*-th channel is considered as artifact.

Determination of the MEG channels mask

The mask is an array of zeros and ones $w_i \in \{0,1\}$, $i = \overline{1,N}$, where *N* is total number of channels. The ones correspond to active channels. Mask can be determined only in the window «MEG-Analysis». In the menu item «Mask–…» one of the fourteen types of masks can be selected.

«Mask–Manual…» calls the dialogue in which a set of the channels can be specified, e.g. 1-5,7-49,51,52,54-148.

«Mask–Zeros» and «Mask–Ones» switch all channels off and on, correspondingly. «Mask–Reverse» calculates the difference between mask of ones and current mask.

In all other types of mask the total number of active channels can be specified in the menu item «Mask–Capacity…».

«Mask–Nearest» establishes the mask from channels closest to the center of mass of current mask.

«Mask–Minimal» and «Mask–Maximal» activate channels with corresponding instant values of the magnetic field.

«Mask–Dipole» activates channels with minimal and maximal instant values of the field in equal quantities.

«Mask–Left», «Mask–Right», «Mask–Front», «Mask–Back», «Mask–Upper» and «Mask–Lower» determine masks from channels located in corresponding regions of the helmet.

Two-dipole model can be used to address the inverse problem. Each dipole (primary and secondary) has its own mask for the selection of active channels. So, in fact, there are two masks: primary and secondary. One can switch between them by clicking the right mouse button at the box «Channel mask». The box «Multichannel MEG» will demonstrate only the time courses of channels, included in primary mask. It is possible to build both masks either from the «Mask–…» menu or by clicking the left mouse button at the particular channel. Each click changes the channel's state to the opposite (active or passive). Clicking the right button at the channel shows its number. If the interactive zooming in the «MEG-Analysis» window is inactive, one can choose the instant of time in the box «Multichannel MEG» by dragging the movable vertical line with the mouse. In this case, the box «Input field pattern» will change correspondingly, showing the instant map of the magnetic field. This magnetic field will be used to solve the inverse problem on the set of active channels.

THE «MEG-Function» WINDOW

This window is intended for processing the one-dimensional time series in order to interactively build a set of triggers. These triggers represent moments of time for signal averaging and correspond to the repetitions of similar events. If the function is reflecting appropriate features of the event, then selection of some function details (e.g. maxima) can provide averaging triggers. A typical example of such a time series is the recording of the stimulus in experiments with evoked fields. Input data for this window are one- or two-dimensional time series; the output data is a set of triggers and average multichannel MEG fragments.

The block diagram and screenshot of the window «MEG-function» are illustrated in Figures 7 and 8. The window displays two boxes. They show samples of the time series that can be opened from the «File – Open – MEG Function…» menu. The bottom picture is used only when the time series are two-dimensional. If interactive zooming in the «MEG-Function» window is inactive, one can drag the movable horizontal line in the top box with

the mouse. This line's position is used as the cut level «Cut level» in the triggers searching procedure («Build – Triggers…» menu). The «Tools – Fourier Transform» menu opens a new window that displays the amplitude spectrum obtained as a result of the Fourier transform.

Fig. 7. Block diagram of the «MEG-Function» window.

Generating time series from multichannel MEG

It is possible to construct a time series $f(t)$ from the «Build–Function–…» menu. The MEG will be taken from the directory specified by the user.

The following time series can be generated:

- One channel to be used as time series is selected through «Build–Function–Channel…» menu: $f_1(t) = B_i^0(t)$, $i \in \overline{1, N}$, $t = \overline{1, T}$, where $B_i^0(t)$ – is magnetic induction in *i*-th channel, N is total number of channels, *T* is the MEG duration.
- The MEG amplitude averaged over the channels is produced through «Build–Function–Amplitude…» menu: $f_2(t) = \sqrt{\frac{\sum_{i=1}^{N} w_i \left(B_i^0(t)\right)^2}{\sum_{i=1}^{N} w_i}}$, $t = \overline{1, T}$, where w_i are the weights of the channels (sensors' reliability). In general, a weight can be any number from 0 to 1, but actually only 0 or 1 are used.
- The MEG power averaged over the channels is build by «Build–Function–Power…» menu: $f_3(t) = \frac{\sum_{i=1}^{N} w_i \left(B_i^0(t)\right)^2}{\sum_{i=1}^{N} w_i}$, $t = \overline{1, T}$.
- The projection onto the model magnetic field is calculated by «Build–Function–Projection…» menu: $f_4(t) = \sum_{i=1}^{N} w_i B_i^0(t) B_i$, $t = \overline{1, T}$, where the model magnetic field is a MEG generated from dipoles («Output field pattern» in the «MRI Analysis» window), and B_i is the normalized distribution of magnetic induction with zero mean: $\sum_{i=1}^{N} w_i B_i = 0$, $\sum_{i=1}^{N} w_i (B_i)^2 = 1$.
- The normalized projection onto the model magnetic field is produced through «Build–Function–CorrCoef…» menu: $f_5(t) = \frac{\sum_{i=1}^{N} w_i B_i^0(t) B_i}{\sqrt{\sum_{i=1}^{N} w_i \left(B_i^0(t)\right)^2}}$, $t = \overline{1, T}$.

– The projection onto the MEG template is build by «Build–Function–Projection-2…» menu): $f_6(t)=\sum_{i=1}^{N} w_i \sum_{s=1}^{T_1} B_i^0(t+s-1)B_i^1(s)$, $t=\overline{1, T-T_1+1}$, $T \geq T_1$, where MEG template $B_i^1(t)$ is an MEG fragment of length T_1 shown in the «Multichannel MEG» part of the «MEG-Analysis» window.

– The normalized projection onto the MEG template is calculated through «Build–Function–CorrCoef-2…» menu:

$$f_7(t)=\frac{\sum_{i=1}^{N} w_i \sum_{s=1}^{T_1} B_i^0(t+s-1)B_i^1(s)}{\sqrt{\sum_{i=1}^{N} w_i \sum_{s=1}^{T_1} \left(B_i^0(t+s-1)\right)^2}\sqrt{\sum_{i=1}^{N} w_i \sum_{s=1}^{T_1} \left(B_i^1(s)\right)^2}}, \; t=\overline{1, T-T_1+1}, \; T \geq T_1.$$

Generating sets of triggers for averaging

Triggers are the time points to be used in signal averaging, producing a template. In order to build the set of triggers one must construct one of the time series described above. After opening this time series, one should address the «Build–Triggers…» menu. Through the opening dialog box, the following parameters can be set:

– Search method – method for searching triggers (using maxima or minima points);
– Cut level – the cutoff level;
– Min step – minimal interval between neighboring triggers.

Using the maxima points, the triggers are put at the moments when the samples of the time series are exceeding the cutoff level. In addition, the minimal distance between the triggers is kept. The case of minima is similar, differing only in the fact that time series are smaller than cutoff level.

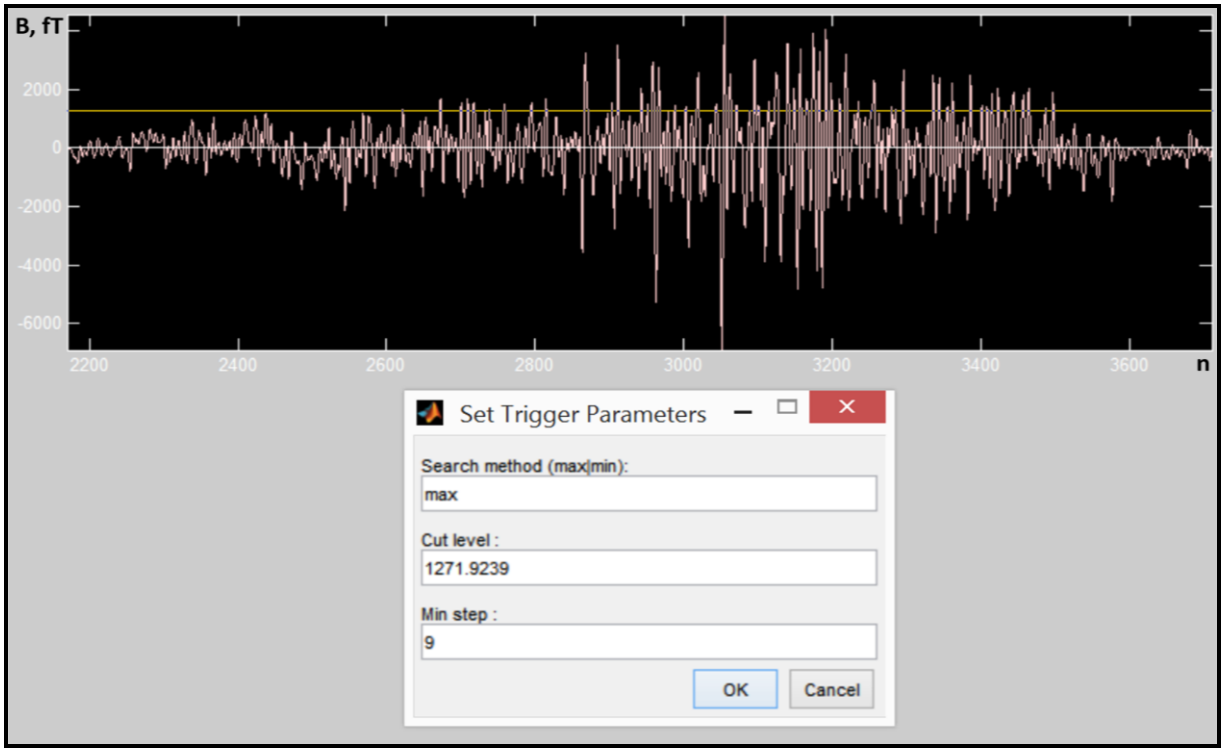

Fig. 8. Building the set of triggers for averaging. The yellow horizontal line shows the cutoff level, the dialog box determines the feature of the signal as a maximum of channel 102, step between triggers as 9 data points.

Building a MEG template

The MEG template can be produced through the «Build–Template…» menu after opening the file containing the set of triggers. Through the opening dialog box, the template length and trigger position can be set. The template will be generated by averaging from the specified MEG folder, and saved in the file.

The box «Time series 1» in Fig.8 illustrates selection of the cut level for the extraction of signal by averaging. Moments of the abnormally high activity in the channel 102 were selected as a signal features. In our previous articles a similar approach was used to extract pathological spontaneous activity in subjects with tinnitus.

THE «MRI-Analysis» WINDOW

This window provides a combined representation of the MEG data, magnetic resonance image (MRI), and functional tomogram (FT). From this window, forward and inverse problems are solved and solutions are also represented in the MRI.

The input data can be:

- head MRI of the subject;
- magnetic field pattern, obtained from the instant MEG values;
- functional tomogram of the subject in the particular experiment.
- The output data are:
- forward problem solution;
- inverse problem solution;
- functional tomogram represented over the MRI.

The block diagram of this window is shown in Figure 9, typical views during the data processing are shown in Figures 10 and 11.

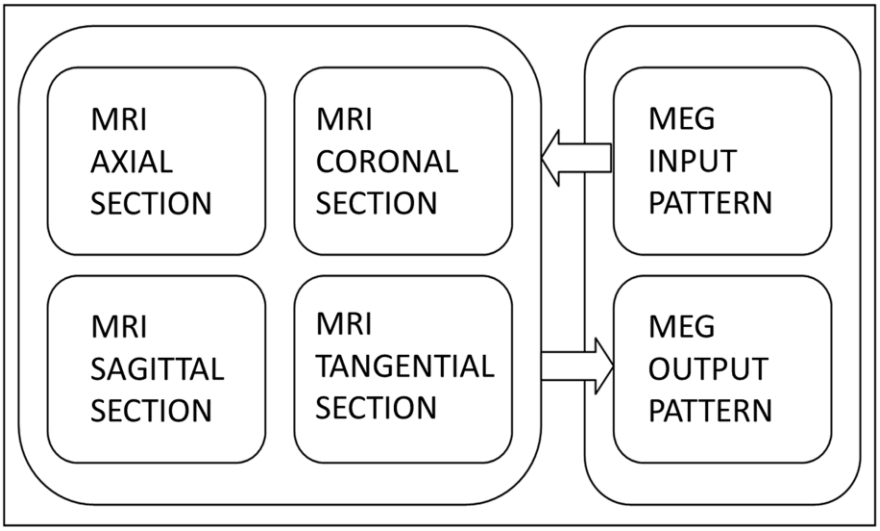

Fig. 9. Block diagram of the window «MRI-Analysis».

The window displays six boxes arranged as a 2×3 matrix. The four boxes on the left represent MRI views. Three standard tomographic sections of the head (coronal, axial and sagittal) passing through the primary dipole are shown in the first three boxes. In the fourth box the tangential section through the same dipole is presented. This section is orthogonal to the radial vector, connecting the model dipole with the center of the conducting sphere. The magnetoencephalograph records only the field from a dipole with a moment, lying in the tangential section plane. If the zooming option in the «MRI-Analysis» window is inactive, one can manipulate the direction and moment of the primary dipole in the tangential box. Left-click at the tangential section changes the moment of this dipole. Right-click at the

tangential section changes the active dipole if a two-dipole model was chosen («Dipole–Number–2» menu). Left-click at one of the tomographic sections of the head changes the position of the primary dipole.

MEG data are shown in the two boxes on the right. The top box is constructed from the field values of an open MEG for a selected moment of time. The bottom box is constructed from the field values calculated from the specified positions and moments of the dipoles, or from the inverse problem solution. The «Options–Mapping» menu enables one to choose the type of a field presentation. This can be an ordinary diagram or an amplitude mapping. The number of a particular MEG channel can be viewed by the right-click over it. The time moment can be changed using the small horizontal slider at the top right of the window, or through the «Deck–…» menu.

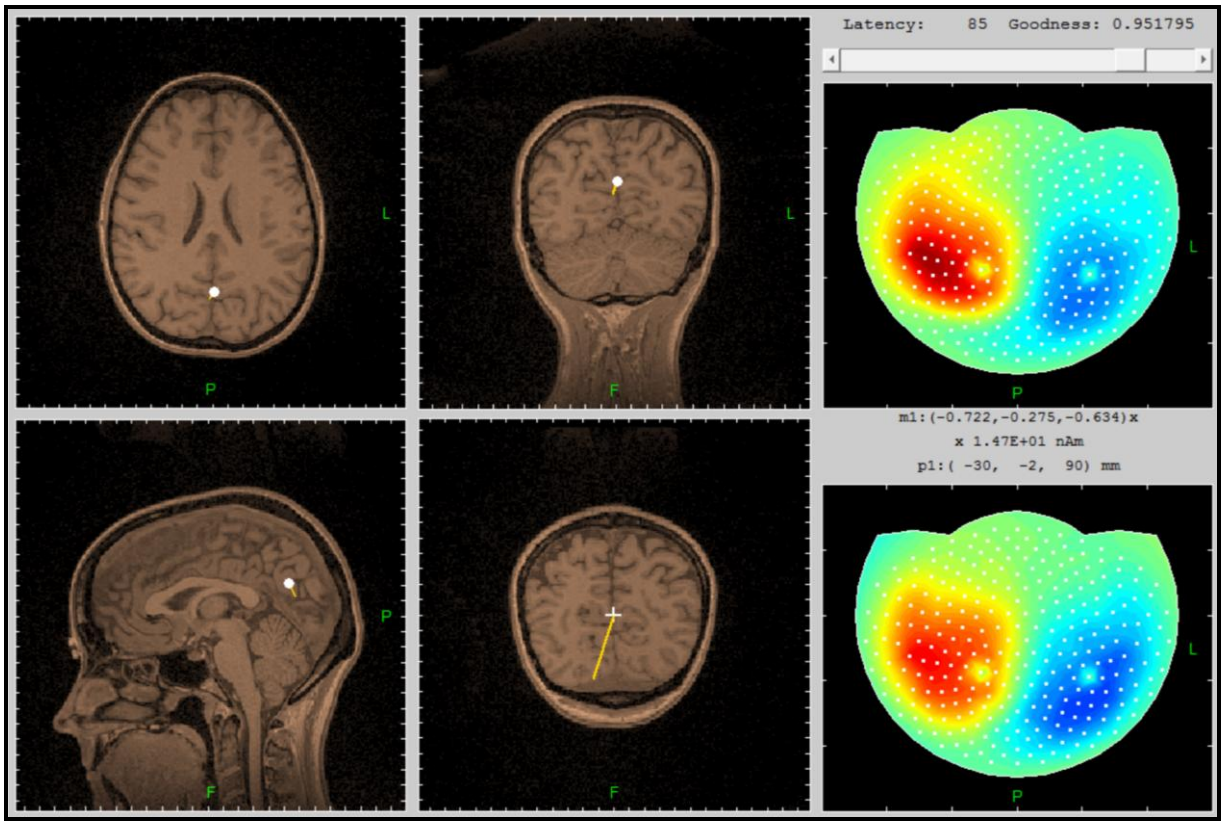

Fig. 10. Typical view of the window «MRI-Analysis». The position and direction of the dipole correspond to the inverse problem solution for the upper right field map. Note, that the goodness of fit is 0.95 of 1.

The forward problem solution

The forward problem of magnetic encephalography consists in finding the magnetic field generated by given sources. The sources of magnetic activity in the brain can be simulated by equivalent current dipoles. Each dipole is characterized by two vectors: $\mathbf{r}_0$ which is the radius-vector of the dipole (dipole location) and $\mathbf{Q}$ which specifies the direction and amplitude of the dipole (dipole moment). To calculate the magnetic induction on the sensors surface use is made of the model of a current dipole in a conducting sphere [29]. For a sensor of the magnetic field occurring at point $\mathbf{r}$ and having direction $\mathbf{n}$, the equation is written as:

$$B(\mathbf{r}_0, \mathbf{Q}) = \frac{\mu_0}{4\pi F^2}\left(\left(F(\mathbf{Q}\times\mathbf{r}_0) - (\mathbf{Q}\times\mathbf{r}_0, \mathbf{r})\nabla F\right), \mathbf{n}\right),$$

$$\text{where } F = a\left(ar + r^2 - (\mathbf{r}_0, \mathbf{r})\right),$$

$$\nabla F = \left(a^2 r^{-1} + a^{-1}(\mathbf{a},\mathbf{r}) + 2a + 2r\right)\mathbf{r} - \left(a + 2r + a^{-1}(\mathbf{a},\mathbf{r})\right)\mathbf{r}_0,$$

$$\mathbf{a} = \mathbf{r} - \mathbf{r}_0,\ a = |\mathbf{a}|,\ r = |\mathbf{r}|,\ |\mathbf{n}| = 1,\ \mu_0 = 4\pi \cdot 10^{-7}.$$

The solution of the forward problem is represented in the box «MEG output pattern», while the positions and moments of the dipoles are typed on the middle right of the window.

The inverse problem solution

The inverse problem solution in MEG addresses the finding of the magnetic field sources from the known values of magnetic induction at some sensors on the head surface. To solve this problem, the following function depending on the magnetic field sources is minimized

$$f = \sum_{i=1}^{N} w_i \left(B_i - B_i^0\right)^2 \to \min .$$

Here B_i^0 are the values of the magnetic induction measured by the sensors, B_i are the relevant values found from the magnetic field sources obtained, w_i are the sensors' weights, and N is the number of sensors.

Provided with the initial guess, the dipoles' location is determined by standard mathematical methods designed for searching the local minimum of the function of several variables. Since in this case the information on the derivatives of the function being minimized is difficult to obtain, the zero-order methods were selected. Namely, the Nelder-Mead simplex method [30] is used for minimization.

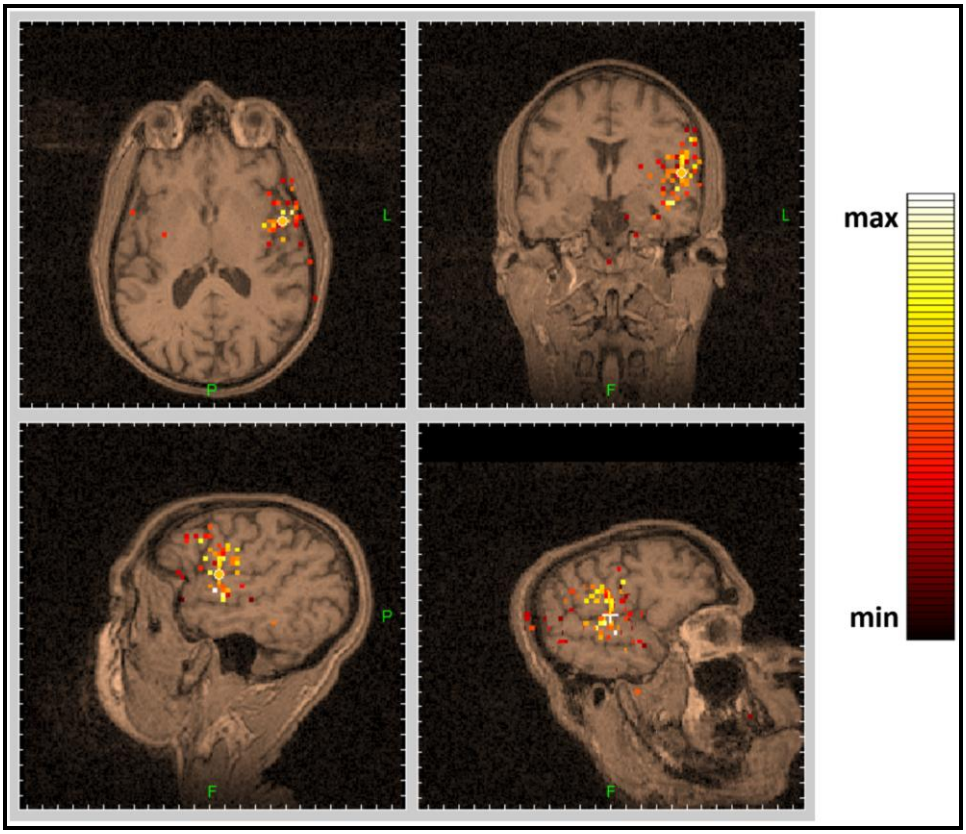

Fig. 11. Representation of the functional tomogram over the MRI. All sources in the frequency band from 65 to 75 Hz are shown, corresponding to the activity burst, discussed in [31, 32]. Insertion shows the legend for relative energy of the sources at the FT.

Notice that the error function depends only on $3N_d$ variables, where N_d is the number of dipoles. These variables determine the dipoles' location. Knowing the dipoles' location and

taking into account that magnetic induction depends linearly on the dipole moments, the latter can be found by solving a relevant system of linear equations.

The quality of the solution («Goodness» in the top right of the window «MRI Analysis» window) is estimated as

$$G = 1 - \frac{\sum_{i=1}^{N} w_i \left(B_i - B_i^0\right)^2}{\sum_{i=1}^{N} w_i \left(B_i^0\right)^2}.$$

The solution of the inverse problem is represented at the box «MEG output pattern», while the positions and moments of the dipoles are typed in the middle right of the window.

Representation of the functional tomogram

The functional tomogram (FT) is defined as a 3-dimensional map of the energy produced by all sources located at a given point in space. It is calculated by outer programs [23, 24] or obtained from other experiments. The software MEGMRIAn provides two interfaces to study functional tomograms together with MRI. One of them is realized as a conjugated representation of the FT and MRI in the window «MRI+FuncTomo». The representation of the FT over the MRI in the window «MRI-analysis» can be seen at Figure 11.

THE «MRI+FuncTomo» WINDOW

This window provides a conjugated parallel representation of the MRI and functional tomogram (FT) as given in [23, 24]. Both objects are shown in the same space, connected by the position of the cursor (Figure 12).

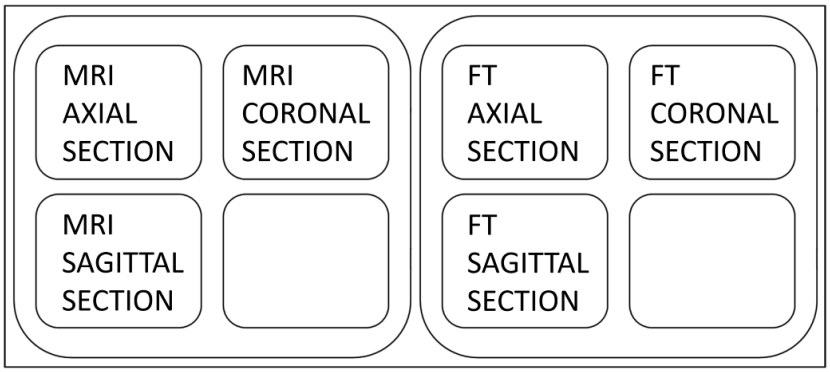

Fig. 12. Block diagram of the «MRI+FuncTomo» window.

The input data are:

- MRI of the subject;
- functional tomogram of this subject in the particular experiment.

The output data are functional tomogram represented side by side with the MRI. The screenshot of the window «MRI+FuncTomo» is illustrated in Figure 13.

Figure 13 shows the functional tomogram, conjugated with the MRI of the same subject. Corresponding sections of the both tomograms are shown, going through the same point in space (Fig.13, white circle).

The functional tomogram along with the MRI can be utilized in the following ways:

- The position in space of the MRI can be selected, corresponding to some anatomical region of interest in the brain. The same position in space of the functional tomogram will show relative activity of this region in the given frequency band.
- Selection of the particular region in space of the functional tomogram makes it possible to determine the anatomical meaning of this phenomenon, by finding the corresponding position in space of the MRI.

Parallel conjugated representation of the FT and MRI makes it possible to study these objects in details not covered by each other. Note, that zooming is also performed simultaneously in both the MRI and FT spaces.

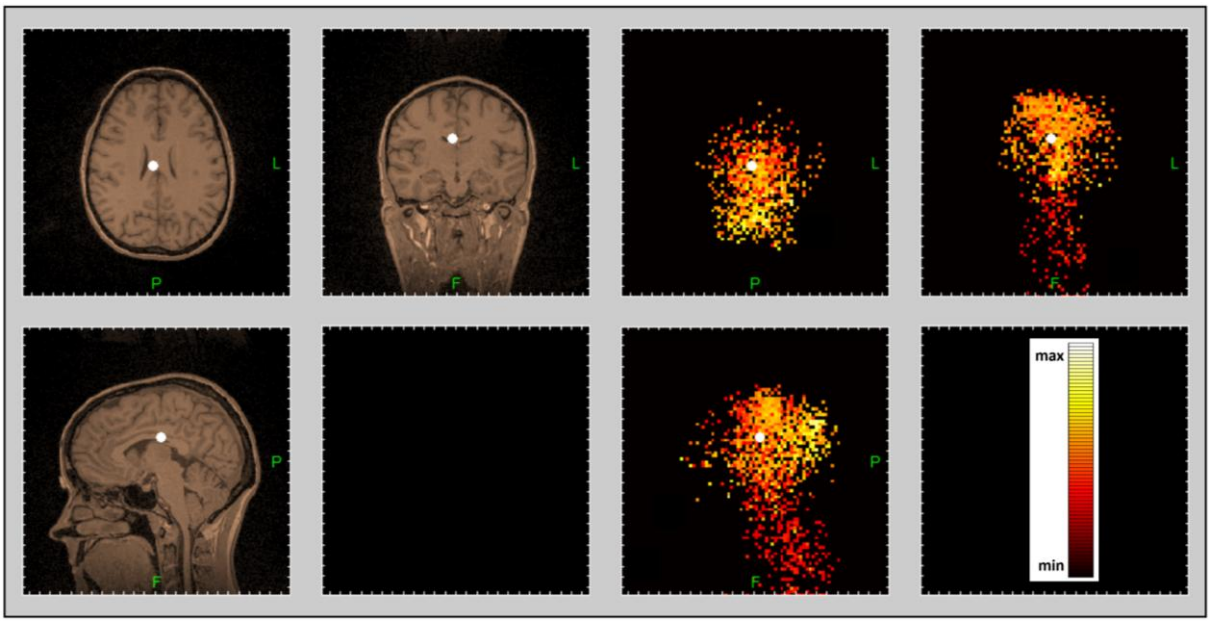

Fig. 13. Typical view of the «MRI+FuncTomo» window showing corresponding sections crossing at the same point (white circle). For the functional tomogram (right) all sources in the frequency band from 0.002 to 100 Hz are shown. Insertion shows the legend for relative energy of the sources at the FT.

CONCLUSIONS

The software developed in this study integrates methods widely used in encephalography with new approaches. Using a graphical user interface and realistic head model, the MEGMRIAn package makes it possible to perform the full cycle of the computational experiment on MEG data.

Development of the software has been carried out by including of new windows and functions of data processing. The software package is under further development to allow calculations through a web-interface similar to [33, 34].

The study was partly supported by the Russian Foundation for Basic Research (grants 13-07-00162, 13-07-12183, 14-07-00636, 14-07-31309), by the CRDF Global (USA) (grants CRDF RB1-2027 and RUB-7095-MO-13) and by the Program 43 for Fundamental Research of the Russian Academy of Sciences.

REFERENCES

1. Hämäläinen M., Hari R., Ilmoniemi R.J., Knuutila J., Lounasmaa O.V. Magnetoencephalography - theory, instrumentation, and application to noninvasive studies of the working human brain. *Rev. Mod. Phys*. 1993. V. 65. P. 413–497. DOI: http://dx.doi.org/10.1103/RevModPhys.65.413.
2. Mosher J.C., Lewis P.S., Leahy R.M. Multiple dipole modeling and localization from spatio-temporal MEG data. *IEEE Transactions on Biomedical Engineering*. 1992. V. 39. № 5. P. 541–557.

3. Baillet S., Friston K., Oostenveld R. Academic software applications for electromagnetic brain mapping using MEG and EEG. C*omputational intelligence and neuroscience.* 2011. V. 2011. Article ID 972050. DOI: http://dx.doi.org/10.1155/2011/972050.
4. Oostenveld R., Fries P., Maris E., Schoffelen J.-M. FieldTrip: open source software for advanced analysis of MEG, EEG and invasive electrophysiological data. *Computational intelligence and neuroscience*. 2011. V. 2011. Article ID 156869. DOI: http://dx.doi.org/10.1155/2011/156869.
5. Tadel F., Baillet S., Mosher J.C, Pantazis D., Leahy R.M. Brainstorm: a user-friendly application for MEG/EEG analysis. *Computational intelligence and neuroscience.* 2011. V. 2011. Article ID 879716. DOI: http://dx.doi.org/10.1155/2011/879716.
6. Aguera P.-E., Jerbi K., Caclin A., Bertrand O. ELAN: A software package for analysis and visualization of MEG, EEG, and LFP signals. *Computational intelligence and neuroscience*. 2011. V. 2011. Article ID 158970. DOI: http://dx.doi.org/10.1155/2011/158970.
7. Campi C., Pascarella A., Sorrentino A., Piana M. Highly automated dipole estimation (HADES). *Computational intelligence and neuroscience*. 2011. V. 2011. Article ID 982185. DOI: http://dx.doi.org/10.1155/2011/982185.
8. Gramfort A., Papadopoulo T., Olivi E., Clerc M. Forward field computation with open MEEG. *Computational intelligence and neuroscience*. 2011. V. 2011. Article ID 923703. DOI: http://dx.doi.org/10.1155/2011/923703.
9. Sudre G., Parkkonen L., Bock E., Baillet S., Wang W., Weber D.G. rtMEG: a real-time software interface for magnetoencephalography. *Computational intelligence and neuroscience*. 2011. V. 2011. Article ID 327953. DOI: http://dx.doi.org/10.1155/2011/327953.
10. Peyk P., Cesarei A.D., Junghöfer M. ElectroMagnetoEncephalography software: overview and integration with other EEG/MEG toolboxes. *Computational intelligence and neuroscience*. 2011. V. 2011. Article ID 861705. DOI: http://dx.doi.org/10.1155/2011/861705.
11. Dalal S.S., Zumer J.M., Guggisberg A.G., Trumpis M., Wong D.D.E., Sekihara K., Nagarajan S.S. MEG/EEG source reconstruction, statistical evaluation, and visualization with NUTMEG. *Computational intelligence and neuroscience*. 2011. V. 2011. Article ID 758973. DOI: http://dx.doi.org/10.1155/2011/758973.
12. Ustinin M.N., Kronberg E., Filippov S.V., Sychev V.V., Sobolev E.V., Llinás R. Kinematic visualization of human magnetic encephalography. *Mathematical Biology and Bioinformatics.* 2010. V. 5. № 2. P. 176–187. URL: http://www.matbio.org/downloads_en/Ustinin2010(5_176).pdf (accessed 03 December 2014).
13. Suk J., Ribary U., Cappell J. Yamamoto T., Llinás R. Anatomical localization revealed by MEG recordings of the human somatosensory system. *Electroenceph. Clin. Neurophysiol.* 1991. V. 78. P. 185-196.
14. Ribary U., Llinás R., Lado F., Mogilner A., Jagow R., Nomura M., Lopez L. The spatial and temporal organization of the 40-Hz response in human brain: A MEG Study. *Biomagnetism: Clinical Aspects: Proceedings of the 8th International Conference on Biomagnetism, Munster, 19-24 August, 1991*. Eds.: Hoke M., Erne S.N., Okada Y.C., Romani G.L. Elsevier Science Publishers, 1992. (International Congress Series).
15. Sekar K., Findley W.M., Llinás R.R. Evidence for an all-or-none perceptual response: Single trial analysis of magneto-encephalography signals indicate an abrupt transition between visual perception and its absence. *Neuroscience.* V. 206. P. 167-182.
16. Sekar K., Findley W.M., Poeppel D., Llinás R.R. Cortical response tracking the conscious experience of threshold duration visual stimuli indicates visual perception is all or none. *PNAS.* V. 110. P. 5642-5647.

17. Llinás R., Ribary U., Jeanmonod D., Kronberg E., Mitra P. Thalamocortical dysrhythmia: A neurological and neuropsychiatric syndrome characterized by magnetoencephalography. *PNAS.* 1999. V. 96. № 26. P. 15222–15227.
18. Schulman J.J., Cancro R., Lowe S., Lu F., Walton K.D., Llinás R.R. Imaging of thalamocortical dysrhythmia in neuropsychiatry. *Front. Hum. Neurosci.* 2011. V. 5. P. 69. DOI: http://dx.doi.org/10.3389/fnhum.2011.00069.
19. Walton, K.D., Dubois, M., Llinás, R.R. Abnormal thalamocortical activity in patients with Complex Regional Pain Syndrome (CRPS) type I. *Pain.* 2010. V. 150. P. 41-51. DOI: http://dx.doi.org/10.1016/j.pain.2010.02.023.
20. Dedus A.F., Dedus F.F., Makhortykh S.A., Ustinin M.N. Analytical description of multidimensional signals for solving problems of pattern recognition and image analysis. *Pattern Recognition and Image Analysis*. 1993. V. 3. № 4. P. 459–469.
21. Dedus F.F., Makhortykh S.A., Ustinin M.N. A generalized spectral analytical method of data processing for signal processing and image analysis problems. *Pattern Recognition and Image Analysis*. 1996. V. 6. № 1. P. 84–85.
22. Dedus F.F., Dedus A.F., Makhortykh S.A., Ustinin M.N. Application of the generalized spectral-analytic method in information problems. *Pattern Recognition and Image Analysis*. 2002. V. 12. № 4. P. 429–437.
23. Llinás R.R., Ustinin M.N. Frequency-pattern functional tomography of magnetoencephalography data allows new approach to the study of human brain organization. *Front. Neural Circuits*. 2014. V. 8. P. 43. DOI: http://dx.doi.org/10.3389/fncir.2014.00043.
24. Llinás R.R., Ustinin M.N. *Precise Frequency-Pattern Analysis to Decompose Complex Systems into Functionally Invariant Entities*: U.S. Patent. US20140107979 A1. 2014.
25. Korshakov A.V., Polikarpov M.A., Ustinin M.N., Sychev V.V., Rykunov S.D., Naurzakov S.P., Grenbenkin A.P., Panchenko V.Ya. Registration and Analysis of Precise Frequency EEG/MEG Responses of Human Brain Auditory Cortex to Monaural Sound Stimulation with Fixed Frequency Components. *Mathematical Biology and Bioinformatics*. 2014. V. 9. № 1. P. 296-308. URL: http://www.matbio.org/2014/Korshakov_9_296.pdf (accessed 03 December 2014) (in Russ.).
26. Ustinin M.N., Makhortykh S.A., Molchanov A.M., Ol'shevets M.M., Pankratova A.N., Pankratova N.M., Sukharev V.I., Sychev V.V. In: *Computers and supercomputers in biology*. Eds. Lakhno V.D. and Ustinin M.N. Moscow-Izhevsk; 2002. P. 327–348 (in Russ.).
27. Ustinin M.N., Polikarpov M.A., Pankratov A.N., Rykunov S.D., Naurzakov S.P., Grebenkin A.P., Panchenko V.Ya. Comparative Analysis of Magnetic Encephalography Data Sets. *Mathematical Biology and Bioinformatics.* 2011. V. 6. № 1. P. 63–70. URL: http://www.matbio.org/2011/Ustinin2011(6_63).pdf (accessed 03 December 2014) (in Russ.).
28. Lakhno V.D., Isaev E.A., Pugachev V.D., Zaitsev A.Yu., Fialko N.S., Rykunov S.D., Ustinin M.N. Development of Information and Communication Technologies in Pushchino Research Center of the Russian Academy of Sciences. *Mathematical Biology and Bioinformatics.* 2012. V. 7. № 2. P. 529–544. URL: http://www.matbio.org/2012/Lakhno_7_529.pdf (accessed 03 December 2014) (in Russ.).
29. Sarvas J. Basic mathematic and electromagnetic concepts of the biomagnetic inverse problem. *Phys. Med. Biol.* 1987. V. 32. P. 11–22.
30. Lagarias J.C., Reeds J.A., Wright M.H., and Wright P.E. Convergence properties of the Nelder-Mead simplex method in low dimensions. *SIAM Journal of Optimization.* 1998. V. 9. P. 112–147.

31. Pankratova N.M., Ustinin M.N., Molchanov A.M., Linas R. Mathematical interpretation of the switching over between the regimes of electrical activity of the brain. *Biophysics*. 2009. T. 54. № 5. C. 916–920 (in Russ.).
32. Pankratova N.M., Ustinin M.N., Llinás R.R. The Method to Reveal Pathologic Activity of Human Brain in the Magnetic Encephalography Data. *Mathematical Biology and Bioinformatics.* 2013. V. 8. № 2. P. 679–690. URL: http://www.matbio.org/2013/Pankratova_8_679.pdf (accessed 03 December 2014) (in Russ.).
33. Lakhno V., Nazipova N. , Kim V., Filippov S., Zaitsev A., Fialko N. , Tyulbasheva G., Ustinin D., Teplukhin A., Ustinin M. Integrated Mathematical Model of the Living Cell. *Mathematical Biology and Bioinformatics*. 2007. V. 2. P. 361–376. URL: http://www.matbio.org/downloads/Lakhno2007(2_361).pdf (accessed 03 December 2014) (in Russ.).
34. Oplachko E.S., Ustinin D.M., Ustinin M.N. Cloud Computing Technologies and their Application in Problems of Computational Biology. *Mathematical Biology and Bioinformatics.* 2013. V. 8. № 2. P. 449–466. URL: http://www.matbio.org/2013/Oplachko_8_449.pdf (accessed 03 December 2014) (in Russ.).

Received November 21, 2014.
Published December 05, 2014.